1 Abstract

This investigation explored the validity of theoretical models of polymer dynamics relevant to dsDNA, an important biological polymer. A numerical simulation using an Euler integration scheme was used to model a Brownian particle in a harmonic potential, and its validity was verified for a particle in one, two and three dimensional vector spaces by comparison to the theoretical model's mean squared displacement across a range of numbers of particles and duration of simulations. This model was extended to produce a theoretical particle-spring model for the dynamics of a polymer, in order to assess its validity at the molecular scale compared with a freely-jointed chain model, through the variation of the spring constant and number of monomers modelled. It was found that a non-dimensional stiffness to monomer number ratio exceeding 10 gave rise to a close match between the simulated data and the theoretical freely-jointed chain model. The freely-jointed chain model itself, and a worm-like chain model were directly compared to experimental data for the force-extension relationship of λ-phage dsDNA, which was found to be best modelled by the semi-flexibe worm-like chain model.

2 Introduction

Polymer physics plays a very important role in cell biology, with polymer structures such as DNA giving rise to and organism's unique characteristics, and proteins playing functional roles in cells' growth and structure. Protein filaments of the cell's cytoskeleton can fall under three major types - actin filaments, intermediate filaments and actin filaments - which all have differing underlying mechanical properties resulting in their individual roles in the life of the cell. High-stiffness microtubles make up the tracks for intracellular transport, and play a structural role in cell shape, whilst low-stiffness intermediate filaments for fibrous proteins such as keratin, which can provide the anchoring for organelles such as the cell nucleus. Actin filaments play a role in the maintenance of cell shape, and are involved with cells' crawling motion, therefore it is important that these have an intermediate bending stiffness. The stiffness of biological polymers also plays a crucial role in their packing within the volumes that they are limited to. The DNA polymer that makes up the human genome carries an extraordinary amount of information [1], therefore requires a macroscopic contour length giving a millimetre-scale radius of gyration, whilst it is contained in a micrometer-scale nucleus. It is therefore relevant to produce various theoretical models in order to better understand the dynamics of biological polymers, and how these affect the growth, development and behaviour of organisms.

Networks of polymer chains involve large numbers of underlying monomers each existing in a particular microstate, which when connected give rise to an inordinately large number of possible configurations for which the system can take. Theoretical models of polymers therefore make use of a probabilistic approach based on the joint distribution of Brownian particles in contact with a thermostat, and limits on the correlation between links of the chain are imposed in order to analogise the polymers to regimes of the Langevin dynamics governing Brownian particles [2]: stiff polymers can be approximated to a ballistic regime (where particles move in straight lines of constant velocity between collisions) and flexible polymers can be approximated to the diffusive regime (where particle inertia is negligible the area over which its motions covers increases linearly with time).

This study investigates the dynamics of a Brownian particle in a harmonic potential, and its applicability to a model of a polymer as a series of particles interconnected by springs through the use of numerical simulation. Its suitability is assessed through direct comparison to a freely jointed chain model, with a known theoretical solution for the form of its force-extension relationship. This latter model and a worm-like chain polymer model are directly compared to experimental force-extension data for a biological polymer in order to assess their relevance and limitations.

3 Methods

In order to simulate the Brownian particle in a harmonic potential and Force-extension of DNA, it is necessary to use a dimensionless numerical method. Since all systems analysed are based on differential equations to the first order, it was deemed sufficient to use a simple Euler integration scheme, $s(t_{j+1}) = s(t_j) + (t_{j+1} - t_j)\dot{s}(t_j)$, where $s(\dot{t}_j)$ can be written as a function of $s(t_j)$. A python script was used to carry out all simulations.

4 Results and discussions

4.1 Brownian particle in a harmonic potential

4.1.1 Model for a Brownian particle in a harmonic potential

Brownian motion describes the random motion of a small particle which is immersed in a fluid of the same density. The equations of motion for a Brownian particle can be derived through considering the transfer of momentum between particles randomly colliding in such a colloidal system. There are three time scales associated with such a system: the short atomic time scale, describing the time between collisions; the Brownian time scale for particle velocity relaxation, which can be realised as the observer's time resolution; and the relaxation time for a Brownian particle, which can be realised as the characteristic variation of the particle's velocity, or as the time for which the particle diffuses its own characteristic distance (such as a radius). Considering a separation of these time scales, and looking from the perspective of the observer's timescale, the dynamics of a Brownian particle can be described by Langevin's equation [2].

In the case of a free particle, its dynamics can written as

$$0 = -\zeta\dot{\mathbf{r}}(t) + \mathbf{f}_\mathbf{r}(t) \tag{1}$$

where $\mathbf{f}_\mathbf{r}(t)$ is a fluctuating force arising from the random collisions between particles in the system. The first and second moments of this fluctuating force are $E[\mathbf{f}_\mathbf{r}(t)] = 0$ and $E[f_{r,i}(t_1)f_{r,j}(t_2)] = 2\zeta k_B T\delta_{ij}\delta(t_1 - t_2)$ respectively - where $\delta_{ij} = 1 if i = j, 0 otherwise$ and i, j represent the coordinate axes for an N-dimensional space, i.e. x, y, z in the three-dimensional case - defining the fluctuating force as having a Gaussian distribution when we apply the Central Limit Theorem.

A Brownian particle in a harmonic potential has the governing dynamics

$$0 = -\zeta\dot{\mathbf{r}}(t) - k\mathbf{r}(t) + \mathbf{f}_\mathbf{r}(t) \tag{2}$$

where ζ is the friction coefficient, and we can think of the constant k being some equivalent spring constant that results in some restoring force which resists the particle's diffusion away from the origin. For such a particle with a start position defined as the origin of some coordinate system, $\mathbf{r}(0) = 0$, its mean displacement is $E[\mathbf{r}(t)] = 0$. The mean squared displacement for a particle of such dynamics, which gives us information about the range over which the particles have travelled over a given time t, can be shown (see Appendix 1.1 for the full derivation) to be

$$E[\mathbf{r}(t)^2] = \frac{Nk_BT\tau}{\zeta}\left[1 - e^{-\frac{2t}{\tau}}\right] = \frac{Nk_BT}{k}\left[1 - e^{-\frac{2t}{\tau}}\right] \tag{3}$$

for an N-dimensional space. Here, $\tau = \frac{\zeta}{k}$, defining our observer time. In the limit where $t << \tau$, $E[\mathbf{r}(t)^2] \to 0$, since the time is well below the minimum time allowing the observation of a change. As $t >> \tau$, $E[\mathbf{r}(t)^2] \to \frac{Nk_BT}{k}$, which simply gives us the equipartition theorem, since the potential energy for the harmonic oscillator with a relaxation on its velocity (i.e. ignoring kinetic energy) can be written as $\frac{1}{2}kE[\mathbf{r}(t)^2]$, and $\frac{1}{2}kE[\mathbf{r}(t)^2] = \frac{1}{2}Nk_BT$.

4.1.2 Brownian particle simulations

The Euler integration scheme for a free particle can be realised as

$$\mathbf{r}(t_{i+1}) = \mathbf{r}(t_i) + \frac{\Delta t}{\zeta}\mathbf{f}_\mathbf{r}(t_i) = \mathbf{r}_{i+1} = \mathbf{r}(t_i) + \sqrt{2D\Delta t}\mathbf{b}_i \tag{4}$$

where D is the diffusion constant, obtained from the fluctuation dissipation theorem of a particle in Brownian motion [3], and $\mathbf{b}_i$ is a random vector, with a standard Gaussian distribution.

We can therefore similarly write the integration scheme for a particle in a harmonic potential as

$$\mathbf{r}_{i+1} = \mathbf{r}_i \left(1 - \frac{\Delta t}{\tau}\right) + \sqrt{2D\Delta t}\mathbf{b}_i \tag{5}$$

which can be non-dimensionalised by the parameters $\theta = \tau$, $\tilde{t} = t/\theta$, $\lambda = \sqrt{k_B T/k}$, $\tilde{\mathbf{r}}_i = \mathbf{r}(t = i\theta\Delta\tilde{t})/\lambda$, $\epsilon = k_B T$ to yield

$$\tilde{\mathbf{r}}_{i+1} = \tilde{\mathbf{r}}_i(1 - \Delta\tilde{t}) + \sqrt{2\Delta\tilde{t}}\mathbf{b}_i \tag{6}$$

In the non-dimensional case, we also therefore expect to see the mean squared displacement become $E[\tilde{\mathbf{r}}(\tilde{t})^2] = N(1 - e^{-2\tilde{t}})$, where N is the number of dimensions of the space. This is expected to tend to zero for small dimensionless time, and to N for large dimensionless time (i.e. a small or large number of iterations of the simulation).

The validity of the above analysis was verified by simulating for a system of particles of specified particle number and number of iterations of the simulation, in one, two and three dimensions, in keeping with possible real-life systems. The results of this simulation for the case of 1000 particles and 5000 iterations is depicted in Figure 1.

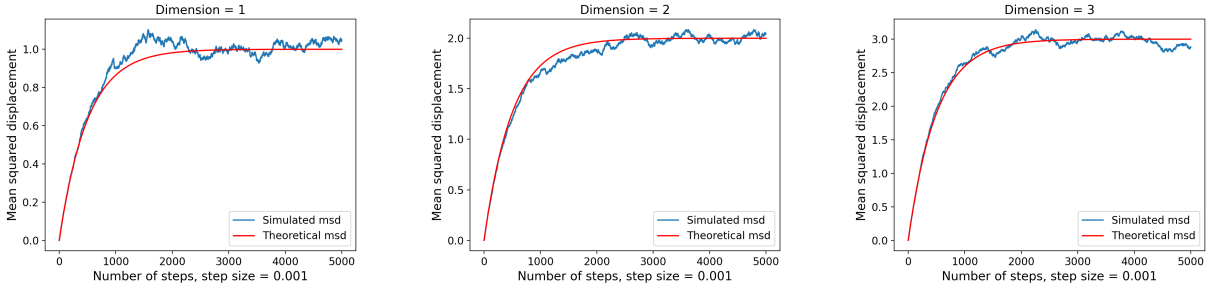

(a) One-dimensional system (b) Two-dimensional system (c) Three-dimensional system

Figure 1: Comparison of the theoretical evolution of the mean squared displacement of a Brownian particle in a harmonic potential with a numerical simulation, using a system of 1000 particles and 5000 iterations

As indicated in 2, for this particular system, the errors in two and three-dimensional systems spread to slightly larger values than those of the one-dimensional system, however the distribution of errors was similar across the three. The effects of the number of particles on the error of the simulation compared to the theory were further studied. For the purpose of simplicity, systems of 1, 10, 50, 100, 250, 500, 750, 1000, 1500, 2000 and 5000 particles were studied each for 2500 iterations of the simulation (the value near to which we see the exponential plateau), and the particle number was plotted against the mean value of the error. Figure 3 shows that the mean error drops rapidly in what appears to be an exponential relationship with the number of particles, regardless of the number of dimensions for which the system sits in. Further analysis is warranted in order to calculate the regression of this relationship, and is outside the scope of this report at present.

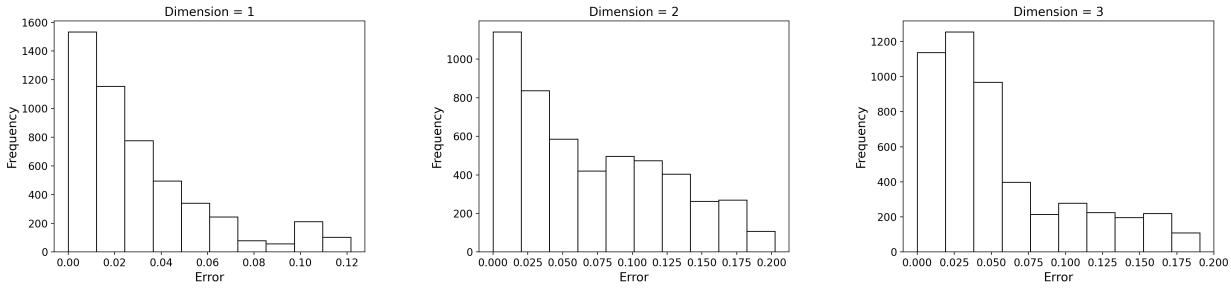

(a) One-dimensional system (b) Two-dimensional system (c) Three-dimensional system

Figure 2: Distribution of the absolute errors between the simulated and theoretical systems for a Brownian particle in a harmonic potential, using a system of 1000 particles and 5000 iterations

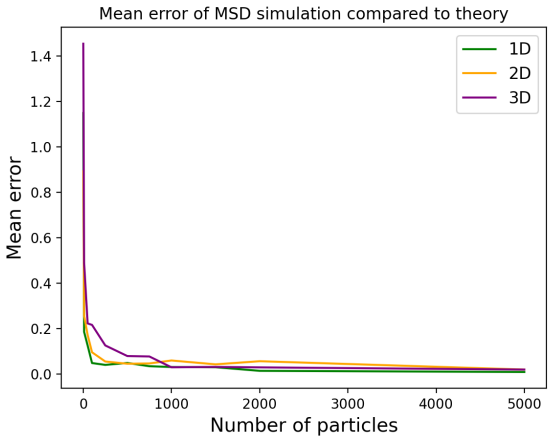

Figure 3: Variation of the mean error between the theoretical and simulated mean squared displacement of a Brownian particle in harmonic potential, as the number of particles simulated increases from 1 to 5000

4.2 Force-extension of DNA

4.2.1 Model for the DNA polymer

For the particle-spring model for a polymer, as in Figure 4, the equation of motion for a particle taking the positional vector $\mathbf{r}_n$, where $n \neq 0, 1$, can be written as

$$\zeta \dot{\mathbf{r}}_n = \kappa \left(\left(\mathbf{r}_n - \mathbf{r}_{n+1} - l \frac{\mathbf{r}_n - \mathbf{r}_{n+1}}{|\mathbf{r}_n - \mathbf{r}_{n+1}|} \right) + \left(\mathbf{r}_n - \mathbf{r}_{n-1} - l \frac{\mathbf{r}_n - \mathbf{r}_{n-1}}{|\mathbf{r}_n - \mathbf{r}_{n-1}|} \right) \right) + \mathbf{f}_n \tag{7}$$

where the second term on the right hand side of Equation 7 represents the force of the particle experienced due to the extension of its attached springs (of natural length l), as a result of the relative displacements of the adjacent particles. Defining the pulling force, $\mathbf{p}$ to be positive in the direction $\mathbf{r}_N - \mathbf{r}_0$, where the number of particles is $N + 1$, at the particle of position $\mathbf{r}_0$, this second term reduces to $\kappa(\mathbf{r}_0 - \mathbf{r}_1 - l\frac{\mathbf{r}_0 - \mathbf{r}_1}{|\mathbf{r}_0 - \mathbf{r}_1|} + \mathbf{p})$. Similarly, this becomes $\kappa(\mathbf{r}_N - \mathbf{r}_{N-1} - l\frac{\mathbf{r}_N - \mathbf{r}_{N-1}}{|\mathbf{r}_N - \mathbf{r}_{N-1}|} - \mathbf{p})$ for the particle at position $\mathbf{r}_N$, with the sign of the force reversing as a result of it being in opposing orientation at this position as compared to at $\mathbf{r}_0$.

Defining the parameters $\lambda = l$, $\theta = \frac{\zeta l^2}{k_B T}$, $\epsilon = k_B T$, $k = \frac{\kappa l^2}{k_B T}$ and introducing the dimensionless terms $\tilde{\mathbf{r}}_{n,i} = \mathbf{r}_{n,i}/\lambda$, $\tilde{t} = t/\theta$, $\tilde{\mathbf{p}} = \frac{\mathbf{p}l}{k_B T}$, the dimensionless Euler integration method for this system (see Appendix 1.2 for full derivation) becomes

$$\tilde{\mathbf{r}}_{n,i+1} = \tilde{\mathbf{r}}_{n,i} - \Delta\tilde{t}\left[k\mathbf{f}(\tilde{\mathbf{r}}_{n,i} - \tilde{\mathbf{r}}_{n-1,i}) + k\mathbf{f}(\tilde{\mathbf{r}}_{n,i} - \tilde{\mathbf{r}}_{n+1,i})\right] + \sqrt{2\Delta\tilde{t}}\mathbf{b}_{n,i} \tag{8}$$

$$\tilde{\mathbf{r}}_{0,i+1} = \tilde{\mathbf{r}}_{0,i} - \Delta\tilde{t}\left[k\mathbf{f}(\tilde{\mathbf{r}}_{0,i} - \tilde{\mathbf{r}}_{1,i}) + \tilde{\mathbf{p}}\right] + \sqrt{2\Delta\tilde{t}}\mathbf{b}_{0,i} \tag{9}$$

$$\tilde{\mathbf{r}}_{N,i+1} = \tilde{\mathbf{r}}_{N,i} - \Delta\tilde{t}\left[k\mathbf{f}(\tilde{\mathbf{r}}_{N,i} - \tilde{\mathbf{r}}_{N-1,i}) - \tilde{\mathbf{p}}\right] + \sqrt{2\Delta\tilde{t}}\mathbf{b}_{N,i} \tag{10}$$

where $\mathbf{f}(\mathbf{a}) = (\mathbf{a} - |\mathbf{a}|^{-1})$.

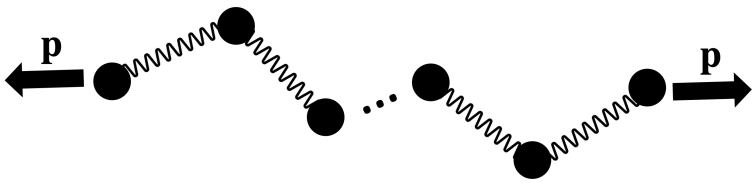

Figure 4: Particle-spring model for a polymer

4.2.2 DNA simulations

The Euler integration scheme described above was used to simulate the relationship between the force applied to the polymer and its resulting extension, and the effects that varying the polymer length (through variation of N) and the non-dimensional spring constant k have on the relationship.

Firstly, the polymer was initialised. A random walk-style simulation, using the simulation for the Brownian particle in a harmonic potential was first used, with the steps taken representing the vectors between

adjacent particles in the polymer, as opposed to a single particle's trajectory in time. For the case of a polymer consisting of 100 particles, and with a dimensionless spring constant of 1, (Figure 5a) the radius of gyration when initialised this way in three dimensions was found to be around 0.28. For a freely jointed chain model for a polymer, we expect its radius of gyration to be equal to $\sqrt{\frac{N}{6}}$, in this case 4.08, therefore further initialisation was carried out by iterating over the Euler method for the particle-spring model with a pulling force of zero, until the polymer's radius of gyration exceeded that of the freely jointed chain model (Figure 5b).

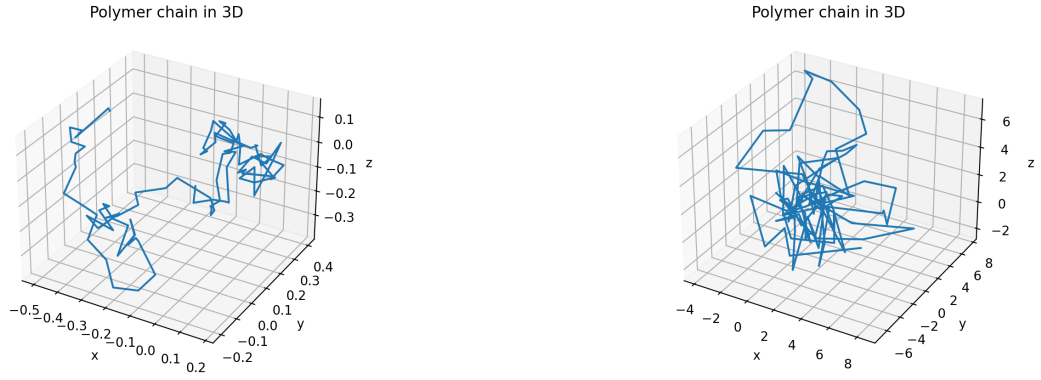

(a) Brownian motion initialisation

(b) Relaxation initialisation with zero force

Figure 5: Initialisation of a polymer for the particle-spring model. Number of particles in the chain N = 100, and dimensionless spring constant k = 1

The number of iterations for the Euler integration scheme for each polymer under a force was chosen to be 1000, given that in analysis of a Brownian particle in a harmonic potential, this was a high enough number of iterations for a relaxation towards a final state, and presented relatively low errors as compared to the theory. The polymer initialised as in Figure 5a was first used to explore the effects of variation of the non-dimensional spring constant k on the force-extension relationship. This was repeated using the initialised polymer as in Figure 5b. For the purpose of simplicity, given the large run times of both the initialisation algorithm and the Euler numerical integration scheme, the same initial polymer chain ($N = 100, k = 1$) was used for all values of k tested to obtain the corresponding force-extension curve, which gives rise to limitations in the simulation. Future simulations may explore the use of more efficient algorithms in order to run the simulations with no ambiguity as the the effects of the start positions, within a realistic time frame.

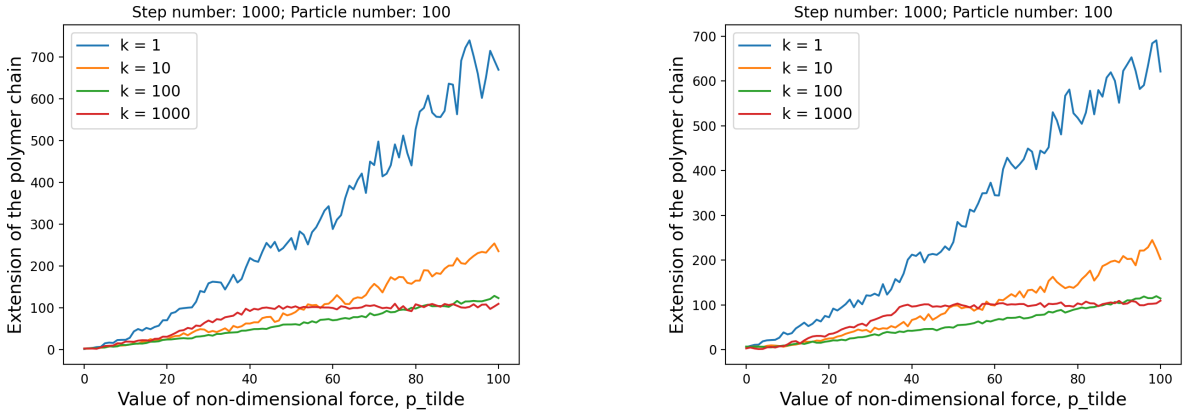

(a) Polymer with Brownian motion initialisation

(b) Polymer with relaxation initialisation

Figure 6: The effect of variation of the non-dimensional spring constant k on the force-extension relationship for a particle-spring modelled polymer of 100 particles

The general trend for variation in the non-dimensional spring constant, k, is that up to an order of magnitude of 10^2, there is a negatively-correlated relationship between the extension of the polymer chain

at a given force, $\tilde{p}$, and the spring constant, as would be expected for a particle-spring system with following classical mechanics. However, as k increases to an order of magnitude of 10^3, the chain's extension exceeds those of $k = 10$ and $k = 100$ at lower force ranges, and a plateau in extension is observed as whilst force continues to increase, indicative of the effects of statistical mechanics and the entropy maximisation-classical energy minimisation trade-off that is characteristic of a system at the molecular scale (discussed in more depth in Section 4.2.3). At this higher $k : N$ ratio, the force-extension relationship is more closely matching to the mean squared displacement-time relationship for a Brownian particle in harmonic potential, suggesting that the similar analogy as for between a Brownian particle in a classical fluid and a freely jointed chain-modelled polymer (as noted in Section 2) can only be applied in the case beyond a certain ratio. There appears to be little effect on the results for the cases of different initialisation methods, likely a characteristic of the large number of Euler integration iterations used in each subsequent simulation, allowing for the relaxation of the chain extensions close to the final equilibrium value.

The effect of the number of particles, N, in the particle-spring chain on its force-extension characteristic was also explored, across an order of magnitude between 10^1 and 10^3, for a fixed value of $k = 100$. There appeared to be very little difference in the force-extension relationships for polymer chains of $N = 100$ and $N = 1000$, which were both quasi-linear, with the same gradient, whereas chain of particle number $N = 10$ had much different behaviour, appearing to exhibit a plateau at the non-dimensional extension of value 10. An initial interpretation of this may be that the similar behaviour of the chains of $N = 100$ and $N = 1000$ is a result of their particle number being closer to the order of magnitude observed in a real polymer, however, through analysis the relative values of k and N, a more rigorous explanation can be realised. Comparing the data of Figure 6 and Figure 7, it is evident that the plateau of extension beyond $\tilde{p} \approx 40$ occurs at a ratio of dimensionless spring constant k particle number N of $10 : 1$, indicating that it is around this value where statistical mechanics begin to play a role, suggesting that there is some threshold for which the particle-spring model becomes valid for modelling polymer dynamics at the molecular scale (further discussed in Section 4.2.3). Future investigation, beyond the scope of this report, could be carried out in order to determine this threshold ratio, for example by investigating the change in error between data points and a linear regression.

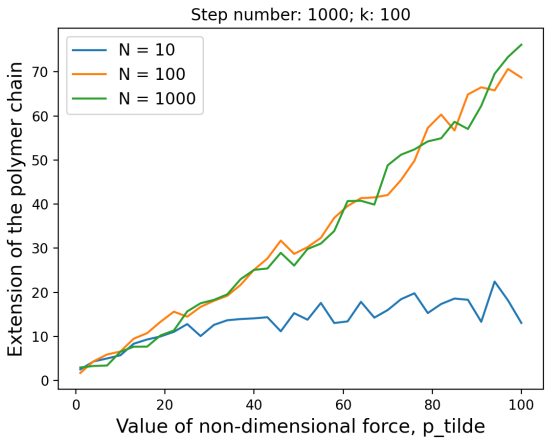

Figure 7: The effects of the number of particles in the particle-spring model for a polymer on the force-extension behaviour

4.2.3 Alternative models

For a freely jointed chain, where the model is similar to that of Section 4.2.1, but the springs are given infinite stiffness (i.e. they are rigid links of fixed uniform length l), we can derive an analytical expression for the polymer chain's force-extension behaviour.

When a pulling force is applied to the polymer chain, a naive expectation which considers only classical mechanics would be that the mean end-to-end displacement $E[\mathbf{R}] = E[\mathbf{r}_n - \mathbf{r}_0]$ would be equal to Nl in order to minimise the potential energy, which is equal to $-p|\mathbf{R}|$, given a magnitude of force p. However, because we are dealing instead with statistical mechanics at the molecular scale, we must also consider maximising entropy. We can imagine entropy as essentially being a force which opposes the pulling force, due to the fact that if the polymer fully extends in the force's direction, it will only exist in one microstate (which would be the case of minimising entropy). Therefore, we must derive some trade-off between minimising potential energy in the classical mechanics sense and maximising entropy.

Keeping the polymer in a thermostat, with a constant force and constant number of particles in the

chain, we can use the partition function

$$Z = \sum_{\{M\}} exp\left[-\frac{(E[M] - \mathbf{p}\cdot\mathbf{R}(M))}{k_B T}\right] \tag{11}$$

to describe the ensemble of the constituent particles at a particular microstate M, where $E[M]-\mathbf{p}\cdot\mathbf{R}(M)$ describes the energy at a given microstate in terms of the classical energy and the potential energy from the pulling of the polymer chain. The classical energy, $E[M]$, is the sum of the kinetic and potential energies, $\sum_{i=0}^{N}\frac{\mathbf{P}_i}{2m}$ (where m is the mass of a particle) and $U(\mathbf{R}_0, ..., \mathbf{R}_N)$ respectively, which are functions of the positions and momenta of the particles that define the microstate $M = \{\mathbf{R}_i, \mathbf{P}_i\}_{i=0,...,N}$. In the case of a freely jointed chain, U imposes the length of the bonds between particles, hence we expect to see a difference in the force-extension curves of the freely jointed chain, and the particle-spring model, since the bond lengths are not fixed in the latter.

The partition function can be thought of as a normalising factor in the probability distribution of the microstates. If we now think of a freely-jointed chain where $\mathbf{r}_i$ describes the vector between particles $i-1$ and i, with a fixed length l and defined relative to some azimuthal axis in spherical coordinates, we can think of the sum in terms of the microstates in Z as being proportional to

$$\int_0^{2\pi} ... \int_0^{2\pi} \int_0^{\pi} ... \int_0^{2\pi} sin(\theta_1)...sin(\theta_N)\, d\theta_1 ... d\theta_N\, d\phi_1 ... d\phi_N$$

where θ_i represents the angle of tilt from the azimuthal axis for each vector and ϕ_i the angle of rotation about it.

If now we define that axis as the axis along which the pulling force is acting, we can simply write that the end-to-end distance of the freely jointed chain is $\sum_{i=1}^{N} lcos(\theta_i)$, which leads us to find that Z is proportional to

$$\prod_{i=1}^{N} \int_0^{2\pi} \int_0^{\pi} sin(\theta_i) e^{\frac{plcos(\theta_i)}{k_B T}}\, d\theta_i\, d\phi_i$$

from which we can find that

$$Z = \left(4\pi \frac{sinh\left(\frac{pl}{k_B T}\right)}{\frac{pl}{k_B T}}\right)^N \tag{12}$$

The mean end-to-end distance can be written as

$$E[R] = \sum_{\{M\}} prob(M)|\mathbf{R}(M)| \tag{13}$$

where $prob(M)$ is the probability of observing a particular microstate, defined as

$$prob(M) = \frac{1}{Z} exp\left[-\frac{(E[M] - \mathbf{p}\cdot\mathbf{R}(M))}{k_B T}\right] \tag{14}$$

and therefore

$$E[R] = e = k_B T \frac{\partial log(Z)}{\partial p} \tag{15}$$

which when we substitute in Equation 12 results in the following force-extension formula for the freely jointed chain:

$$\frac{e}{Nl} = coth\left(\frac{pl}{k_B T}\right) - \frac{k_B T}{pl} \tag{16}$$

Equation 16 can be immediately re-written in dimensionless form, using the parameters specified in Section 4.2.1 as

$$\tilde{e} = N\left(coth(\tilde{p}) - \frac{1}{\tilde{p}}\right) \tag{17}$$

which can be used to compare the polymer model of a freely jointed chain to the particle-spring model.

A polymer with 100 particles, and 1000 iterations of the Euler integration scheme, initialised using the Brownian motion method, (as in 4.2.2) for the particle-spring model at a low and high value of the dimensionless spring constant, $k = 1$ and $k = 100$ respectively was compared with the freely jointed chain model (Figure 8). It is clear that at low values of k (Figure 8a), there is very little alignment with the models, since the freely jointed chain model effectively has links which are springs of infinite stiffness (so the

potential energy-entropy trade-off is omnipresent), whereas at this ratio of $k : N = 1 : 100$ the particle-spring model is dominated by classical mechanics, so is in a linear regime.

At a larger value for k, where $k : N = 10 : 1$, (Figure 8b), the particle-spring model of the polymer exhibits much similar behaviour to the freely-jointed chain model, which is expected since the freely-jointed chain model is essentially the particle-spring model but with springs of infinite stiffness. Discrepancy between the two models at $k = 1000$ is observed at low values of $\tilde{p}$. This is hypothesised to be as a result of a polymers given a lower pulling force requiring a longer time duration in order to reach their equilibriated state. Given a more efficient algorithm, this hypothesis should be explored by running the simulation for a range of step numbers above and below 1000.

A limitation of both models is that neither have a cut-off point for the force which the polymer chain can sustain, simply getting infinitely closer to the plateau extension value, whereas in a true polymer, a maximum extension can be achieved before the pulling energy overcomes the chemical bond energy to break the chain.

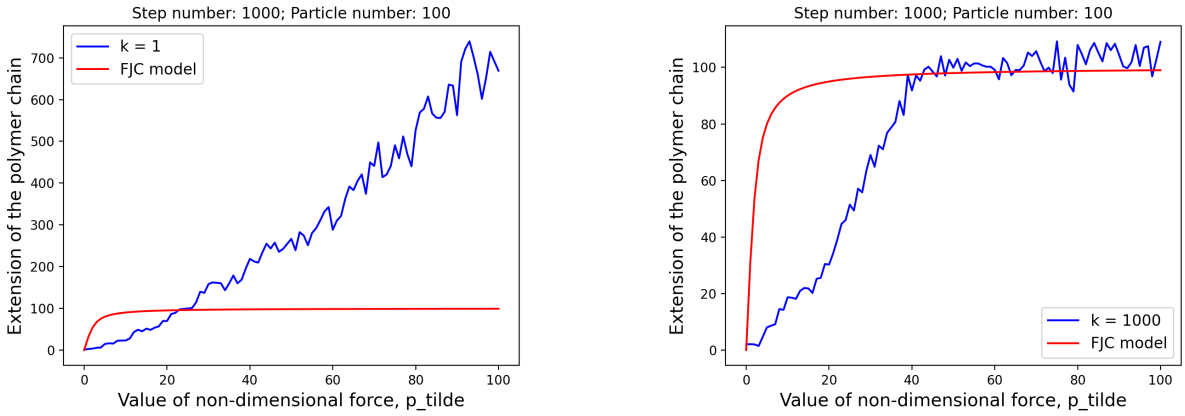

(a) $k = 1$ (b) $k = 1000$

Figure 8: Comparison of the freely jointed chain model for a polymer to the particle-spring model, for a simulation with $N = 100$ particles, and 1000 iteration of the Euler integration scheme at each value of dimensionless force $\tilde{p}$

Another model for a polymer, the worm-like chain, further refines our analytical calculations for the behaviour of a polymer chain by sitting in a regime in which the polymer is not modelled as a stiff rode, or a completely flexible chain, but instead as a semi-flexible rod. For the worm-like chain model, the governing force-extension relationship can be derived as

$$\frac{pl}{2k_BT} = \frac{1}{4}\left(1 - \frac{e}{L}\right)^{-2} - \frac{1}{4} + \frac{e}{L} \tag{18}$$

where L is the contour length, defined as $L = Nl$. Using the same parameters as previously, this can be re-written in the non-dimensional form

$$\tilde{p} = \frac{1}{2}\left(1 - \frac{\tilde{e}}{N}\right)^{-2} - \frac{1}{2}\frac{\tilde{e}}{N} \tag{19}$$

for the purposes of comparison with other models.

To test the validity of these models, real data obtained by Smith et al. (1992), [4], for the force-extension relationship of λ-phage dsDNA polymers was plotted alongside theoretical force-extension relationships of the worm-like chain and freely jointed chain equivalents. The contour length of the λ-phage dsDNA is $L = 32.7\mu m$ and its Kuhn length $l = 106nm$, therefore we can approximate the number of monomers in the chain as $N = L/l = 308$. This experiment was carried out at a temperature of $T = 298K$, with extensions given in nanometers and forces given in pico-Newtons, therefore extensions could be non-dimensionalised by dividing through by 106 and the corresponding required forces non-dimensionalised through multiplication by $\frac{l}{k_BT}$ in the given units.

It is evident in Figure 9 that the shape of the force-extension curve for worm-like chain model is the most appropriate for modelling this polymer structure, suggesting that dsDNA is a semi-flexible polymer. The worm-like chain model, however, has the limitation of modelling a zero extension at a non-zero force, unlike the freely jointed chain model. The experimentally-acquired data has an extension offset compared with both theoretical models explored here, and appears to plateau more rapidly with an increase in force. Neither the

worm-like or freely jointed chain models account for self-interaction in the polymer chain, which can occur due to the effects of particular functional groups of the underlying monomers (such as their electrostatic charges), and has greatest effect at relatively low pulling force. This refinement to polymer models was explored developed by Flory, using Kuhn's concept of excluded volume. Excluded volume models, and the origin of the apparent force-extension curve offset should be further explored before the exact theoretical model for the stiffness and dynamics of λ-phage dsDNA can be determined.

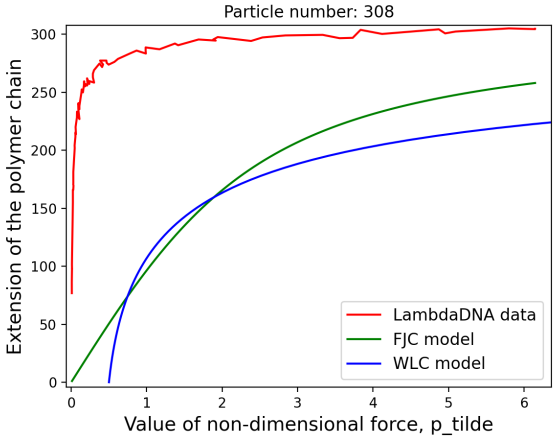

Figure 9: A comparison of the freely jointed chain and worm-like chain models to experimental data for the force-extension of

5 Conclusions

The simulations of this investigation suggest that the force-extension relationship of a polymer model based on a particle-spring model, can be analogous to a Brownian particle in a harmonic potential, and exhibit similarity with a freely jointed chain model, only when the ratio between the model's chosen equivalent for the stiffness constant of links between particles and the number of particles exceeds a threshold governed by the set-up of the model. It is therefore beyond this threshold that the model becomes relevant to modelling a molecular-scale polymer. Although this refinement of a freely jointed chain model to having stretchable links may accommodate the slight allowed stretch of bonds between monomers in a polymer chain, the tendency of the particle-spring model's force-extension curve to that of a freely-jointed chain at such a ratio puts into question the relevance of introducing the finite stiffness constant. The force-extension relationship of the freely jointed chain model itself was shown to not be as closely-matched to experimental data for λ-phage dsDNA as a worm-like chain (semi-flexible) model, however further comparison to experimental data for a variety of biological polymers should be explored to verify the relative validity of different models in a range of contexts.

References

[1] Luis Ceze, Jeff Nivala, and Karin Strauss. Molecular digital data storage using dna. *Nature Reviews Genetics*, 20(8):456–466, 2019.

[2] Bart G de Grooth. A simple model for brownian motion leading to the langevin equation. *American journal of physics*, 67(12):1248–1252, 1999.

[3] Rep Kubo. The fluctuation-dissipation theorem. *Reports on progress in physics*, 29(1):255, 1966.

[4] Steven B Smith, Laura Finzi, and Carlos Bustamante. Direct mechanical measurements of the elasticity of single dna molecules by using magnetic beads. *Science*, 258(5085):1122–1126, 1992.

Appendix 1 - Calculation Details

1.1 Expectation and mean squared displacement for a Brownian particle in a harmonic potential

Writing the equation of motion for the Brownian particle in a harmonic potential as

$$\dot{\mathbf{r}}(t) = -\frac{1}{\tau}\mathbf{r}(t) + \frac{1}{\zeta}\mathbf{f}_{\mathbf{r}}(t) \tag{20}$$

and using the integrating factor $e^{\frac{t}{\tau}}$, with the initial condition $\mathbf{r}(0) = \mathbf{0}$, we can easily find that

$$\mathbf{r}(t) = \frac{1}{\zeta}\int_0^t e^{-\frac{(t-s)}{\tau}}\mathbf{f}_{\mathbf{r}}(t)\,ds \tag{21}$$

therefore

$$E[\mathbf{r}(t)] = \frac{1}{\zeta}\int_0^t e^{-\frac{(t-s)}{\tau}}E[\mathbf{f}_{\mathbf{r}}(t)]\,ds = 0 \tag{22}$$

since $E[\mathbf{f}_{\mathbf{r}}(t)] = 0$. Now if we think about the mean squared displacement of the particle through calculating the second moment between two time steps t_1 and t_2,

$$E[\dot{\mathbf{r}}(t_1)\cdot\dot{\mathbf{r}}(t_2)] = E\left[\int_0^{t_1}\dot{\mathbf{r}}(s_1)\,ds_1\cdot\int_0^{t_2}\dot{\mathbf{r}}(s_2)\,ds_2\right] \tag{23}$$

$$= E\left[\int_0^{t_1}\frac{1}{\zeta}e^{-\frac{(t_1-s_1)}{\tau}}\mathbf{f}_{\mathbf{r}}(s_1)\,ds_1\cdot\int_0^{t_2}\frac{1}{\zeta}e^{-\frac{(t_2-s_2)}{\tau}}\mathbf{f}_{\mathbf{r}}(s_2)\,ds_2\right] \tag{24}$$

$$= \frac{1}{\zeta^2}e^{-\frac{(t_1+t_2)}{\tau}}\int_0^{t_1}\int_0^{t_2}e^{\frac{(s_1+s_2)}{\tau}}E[\mathbf{f}_{\mathbf{r}}(s_1)\cdot\mathbf{f}_{\mathbf{r}}(s_2)]\,ds_1\,ds_2 \tag{25}$$

and since $\mathbf{r}$ can have N dimensions, we can use the expression for the second moment of the random fluctuating force to equate this as

$$E[\dot{\mathbf{r}}(t_1)\cdot\dot{\mathbf{r}}(t_2)] = \frac{1}{\zeta^2}e^{-\frac{(t_1+t_2)}{\tau}}\int_0^{t_1}\int_0^{t_2}e^{\frac{(s_1+s_2)}{\tau}}2N\zeta k_BT\delta(s_1-s_2)\,ds_1\,ds_2 \tag{26}$$

$$= \frac{2Nk_BT}{\zeta}e^{-\frac{(t_1+t_2)}{\tau}}\int_0^{min(t_1,t_2)}e^{\frac{2s}{\tau}}\,ds \tag{27}$$

which, in the limit as $t_1 = t_2 = t$, becomes

$$E[\mathbf{r}(t)^2] = \frac{Nk_BT\tau}{\zeta}\left[1-e^{-\frac{2t}{\tau}}\right] = \frac{Nk_BT}{k}\left[1-e^{-\frac{2t}{\tau}}\right] \tag{28}$$

1.2 Derivation of the dimensionless Euler integration for the particle-spring model

To perform Euler integration for solving Equation 7, we first discretise the time steps, yielding

$$\mathbf{r}_{n,i+1} = \mathbf{r}_{n,i} - \Delta t\left(\frac{\kappa}{\zeta}\left(\mathbf{r}_{n,i}-\mathbf{r}_{n-1,i}-l\frac{\mathbf{r}_{n,i}-\mathbf{r}_{n-1,i}}{|\mathbf{r}_{n,i}-\mathbf{r}_{n-1,i}|}\right)+\frac{\kappa}{\zeta}\left(\mathbf{r}_{n,i}-\mathbf{r}_{n+1,i}-l\frac{\mathbf{r}_{n,i}-\mathbf{r}_{n+1,i}}{|\mathbf{r}_{n,i}-\mathbf{r}_{n+1,i}|}\right)\right)+\frac{\Delta t}{\zeta}\mathbf{f}_{n,i} \tag{29}$$

Using the parameters defined in Section 4.2.1 required to non-dimensionalise the governing equations for the particle-spring model, we can divide Equation 29 through by l to yield

$$\tilde{\mathbf{r}}_{n,i+1} = \tilde{\mathbf{r}}_{n,i} - \Delta t\left(\frac{\kappa}{\zeta}\left(\tilde{\mathbf{r}}_{n,i}-\tilde{\mathbf{r}}_{n-1,i}-\frac{\mathbf{r}_{n,i}-\mathbf{r}_{n-1,i}}{|\mathbf{r}_{n,i}-\mathbf{r}_{n-1,i}|}\right)+\frac{\kappa}{\zeta}\left(\tilde{\mathbf{r}}_{n,i}-\tilde{\mathbf{r}}_{n+1,i}-\frac{\mathbf{r}_{n,i}-\mathbf{r}_{n+1,i}}{|\mathbf{r}_{n,i}-\mathbf{r}_{n+1,i}|}\right)\right)+\frac{\Delta t}{l\zeta}\mathbf{f}_{n,i} \tag{30}$$

Since $\frac{\kappa\Delta t}{\zeta} = \Delta\tilde{t}k$, we can find $\frac{\Delta t}{l\zeta}\mathbf{f}_{n,i} = \frac{\sqrt{2D\Delta t}}{l}\mathbf{b}_i = \frac{\sqrt{\frac{2k_BT}{\zeta}\frac{\zeta l^2}{k_BT}\Delta\tilde{t}}}{l} = \sqrt{2\tilde{t}}\mathbf{b}_i$.

Also, $\frac{\mathbf{r}_{n,i}-\mathbf{r}_{n-1,i}}{|\mathbf{r}_{n,i}-\mathbf{r}_{n-1,i}|}$ can simply have both numerator and denominator divided through by l to give the form of the function $\mathbf{f}(\mathbf{a}) = (\mathbf{a}-|\mathbf{a}|^{-1})$ as shown in the full dimensionless form of Section 4.2.1.